Laser-Induced Fluorescence Observation of Self-Organized Ion Structures Induced by Electrostatic Perturbations

G. Bachet, F. Skiff,* M. Dindelegan, F. Doveil, and R. A. Stern†

Equipe Turbulence Plasma, Laboratoire Physique des Interactions Ioniques et Moléculaires UMR6633 CNRS/Université de Provence, Faculté des Sciences de Saint-Jérôme case 321, Avenue Escadrille Normandie Niemen, F13397 Marseille Cedex 20, France

(Received 29 September 1997)

Effects induced by the propagation of electrostatic perturbations in a low-density collisionless argon plasma are reported. A space-time-velocity resolved laser-induced fluorescence diagnostic shows clearly that the plasma reacts to a steep density perturbation by the formation of self-organized coherent ion structures. [S0031-9007(98)05742-1]

PACS numbers: 52.35.Tc, 52.50.Dg, 52.70.Kz

The mutual interaction of nonlinear and dispersive effects can be observed in the propagation of ion perturbations in a collisionless plasma. Since the theoretical work of Moiseev and Sagdeev [1] who predicted the existence of ion acoustic solitons and shock waves, intensive theoretical and experimental studies have been pursued and important results have been obtained in the turbulence and instabilities associated with the propagation of a density perturbation [2–9]. Among the rich variety of nonlinear structures [10–14], there have been observations of envelope solitons and cavitons or density holes dug in a plasma by high frequency waves and able to trap wave packets. These studies, in progress today [15,16], provide an explanation for the satellite observations of electrostatic ion shock waves [17].

Besides computer simulations, the experimental work that has been done to test the various assumptions of the nonlinear theory has employed mainly Langmuir probes and retarding field energy analyzers. With the rapid progress of optical plasma diagnostics, new tools are available to study nonlinear propagating phenomena. Among laser aided plasma diagnostics [18], the laser-induced fluorescence (LIF) technique [19,20] provides a means to nonintrusively probe plasmas and to measure the ion velocity distribution function (IVDF) with unprecedented resolution in velocity and space. The resolution in velocity is obtained because the Doppler effect is the dominant line-broadening mechanism for a wide range of plasma conditions. Spatial resolution is obtained by collecting the fluorescence light through a viewing volume which intersects the laser beam in a localized region. LIF depends on the fact that laser pumping of a transition will modify the ionic state distributions and, thus, modify the plasma line radiation. Fundamentally, the time resolution of LIF is limited by the lifetime of the upper quantum state of the pumped transition (usually around 10 nsec). In practice, the number of scattered photons is low enough that some form of time averaging is necessary to obtain a distribution function.

To experimentally study propagation, relaxation processes, or instabilities in weakly collisional (low density) plasma, it is necessary to optimize the time resolution. The signal to noise ratio of the fluorescence can be enhanced considerably by averaging over a large number of periods if the observed phenomenon is repeatable. Time resolution can be obtained by using a boxcar averager [21] or a multichannel analyzer synchronized with the observed phenomenon [22,23].

In this paper, after briefly describing the instrumental and diagnostic setup used to generate the density perturbation and to record the ion space time velocity distribution function given by LIF, we show experimental evidence for the presence of a coherent structure excited by a weak density perturbation as it propagates away from an entrance grid.

Experiments are performed in a double plasma device [24,25] with multipolar confinement provided by permanent magnets surrounding the vessel [26]. It consists of two independent hot filament discharge chambers operated with argon gas at a pressure of a few 10^{-4} torr and separated by a plane fine grid held at the floating potential, as sketched in Fig. 1 (top).

In the driver or source plasma, the electron density is equal to a few 10^9 cm^{-3}; in the target plasma, it is of the order of 10^8 cm^{-3}, as measured with plane Langmuir

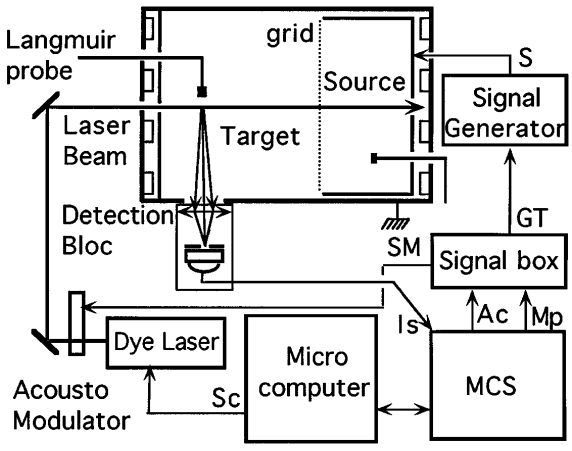

FIG. 1. Time resolved LIF diagnostic setup.

 0031-9007/98/80(15)/3260(4)$15.00

probes. By applying a positive or negative voltage pulse to the open inner conducting cylinder which constitutes the anode of the "driver" plasma, ions can be used to flow into or out of the "target" plasma giving rise, respectively, to a compression or to a rarefactive ion acoustic pulse.

The LIF diagnostic setup, shown on Fig. 1 [27,28], uses a ring dye laser pumped by a cw argon laser. This diagnostic has a spatial resolution of 6 mm^3. To obtain the necessary time resolution, the photomultiplier output is amplified by a wideband amplifier followed by a multichannel scaler (MCS). Two ensembles are independently accumulated and averaged by the MCS. Light from the 461 nm Argon II line is collected alternatively with and without the presence of the laser excitation (at 611 nm). An acousto-optic modulator is used to switch the laser intensity. The difference between these averages defines the LIF signal.

At each spatial location where the measurement is performed, a spectral interval of 12 GHz width is scanned by the dye laser (controlled by the signal "Sc" in Fig. 1) and sampled at 50 points which correspond to 50 ion velocities. For each laser frequency, the MCS output corresponding to the summation of several thousands of scans (10 000 in general) is stored by a microcomputer. In each scan, the first half of 300 temporal channels having a dwell time of 2 μs is filled with the data corresponding to the propagation of the perturbation when the laser is on; the other half contains the data of the plasma emission corresponding to the propagation of the same density perturbation when the laser is off. This allows discrimination of the LIF light from the background emission. Synchronization between the launched perturbation (generated by the signal S), the modulation of the laser, and the acquisition time of the MCS is achieved using a homemade signal box. The acquire (Ac) and middle-pass (Md) outputs of the MCS are used to generate the triggering signal (Gt) for the signal S as well as to generate the control signal for the acousto-optic modulator [22].

The time evolution of the IVDF is then reconstructed using a MATLAB program. To improve the signal to noise ratio, a smoothing of the data is made using a two-dimensional fast Fourier transform to eliminate noise according to the principles of optimal filtering [29].

As stated before, the ion perturbation results from applying to the source plasma discharge potential a periodic rectangular pulse of 150 μs duration with an amplitude varying from -2.5 to 2.5 V. This causes a shock that propagates into the target plasma. The structure of this shock is rather complicated as shown in Fig. 2. Since a wide frequency spectrum of waves can be associated with the applied step function (the voltage transition occurs in a time comparable to the ion plasma period), the spatiotemporal evolution of the perturbation results from the intricate competition of dissipative, dispersive, and nonlinear effects. Figure 2 gives a plot of the IVDF as a function

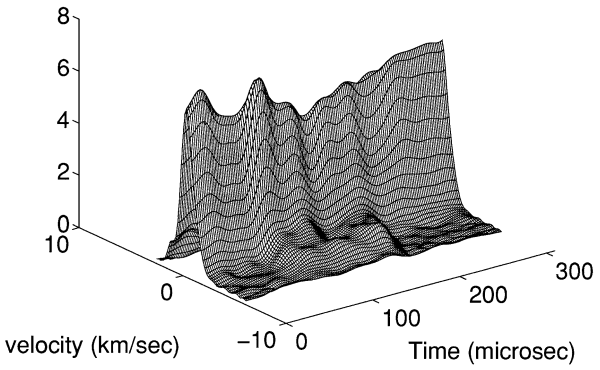

FIG. 2. Time evolution of the ion velocity distribution function.

of time measured at 10 cm from the grid. The main unperturbed ion background distribution can be subtracted and the remaining data give the perturbation of the distribution function induced by the propagation of the shock, as shown in the left column of Fig. 3. On all of the plots, a positive velocity corresponds to propagation toward the entrance grid. On the positive velocity side of the distribution, we observe the formation of a hole, whereas, on the negative velocity side, complex positive ion structures develop. Keeping in mind that the observed structures result from averaging over a large 10 000 independent realizations of the shock, we infer that we are dealing with a highly reproducible and robust phenomenon. An important observation is that a large range of velocities is always associated with the observed spatially localized propagating perturbation. This implies that the self-consistent electric field must be maintaining the observed structures. To confirm this point, we have performed a simple simulation. Starting from the measured contour plot in (v, t) at 5 cm from the grid, we have computed the contour plot that results from the ion ballistic motion taking into account the velocity shear in phase space in the absence of an electric field. A few centimeters away, the structure is completely wiped out.

The spatiotemporal evolution of the perturbation can be most easily studied by using contour plots of the perturbation of the ion velocity distribution function. Figure 3 gives, on the left column, a 3D view of the time evolution of the distribution perturbation, on the middle column, the corresponding contour plots, and, on the right column, the density perturbation measured at a distance of (a) 5 cm and (b) 18 cm from the entrance grid. As the shock propagates away from the gird, the overall perturbation appears to propagate at almost a constant speed. The ion hole keeps essentially the same structure, whereas the ion bumps tend to coalesce to a smaller number of bumps. At 18 cm from the grid, in front of the ion hole, a strong bump of compressed ions appears. Another essential feature of the perturbation is the existence of precursor ions traveling at about twice the ion acoustic speed and that appear as

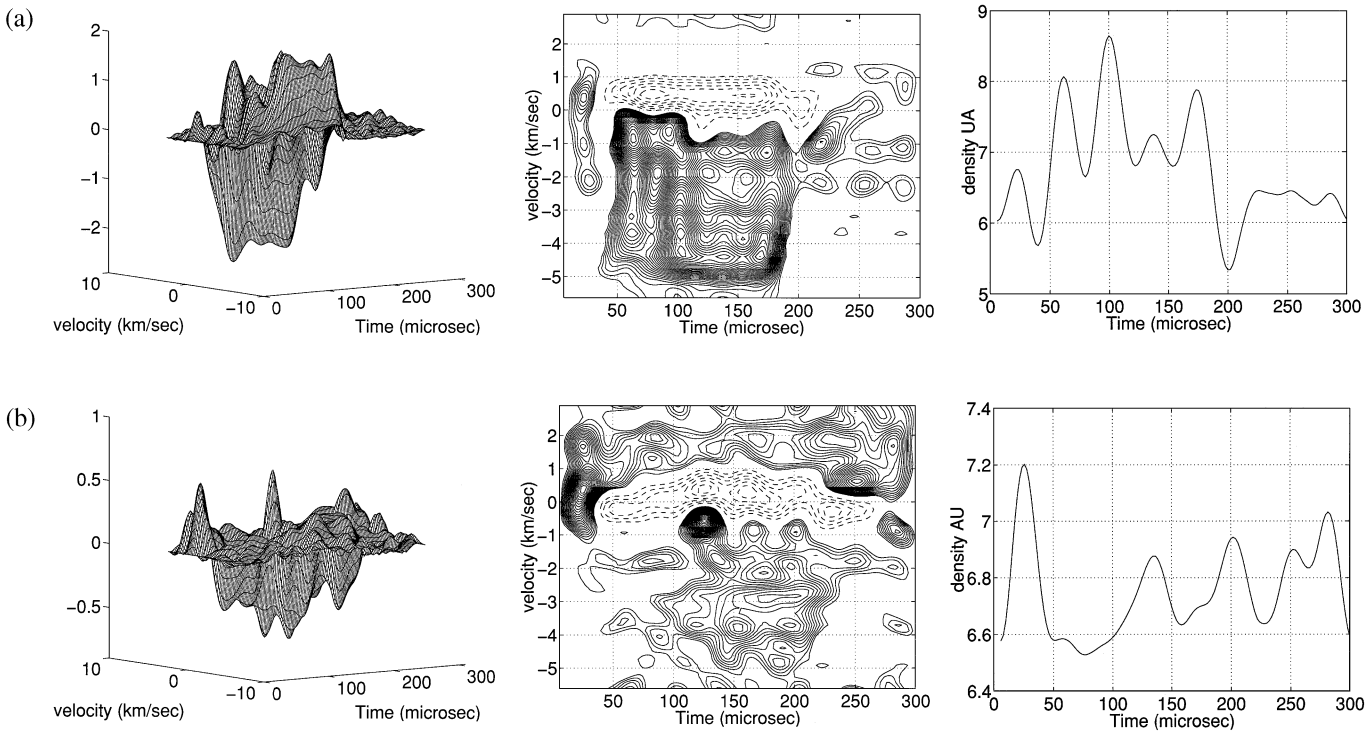

FIG. 3. Left—Time evolution of the perturbation; middle—contour plot in (v, t) plane, dashed line: negative part; right—measured ion density. Measured at (a) 5 cm and (b) 18 cm from the entrance grid.

tongues that propagate before the main structure, as seen on the contour plots. This effect becomes more prominent at higher voltage.

On Fig. 4, we have adopted a different perspective. The distribution perturbation amplitude contours are cross plotted in the (v, x) phase space plane for three different times, at (a) 42 μs, (b) 82 μs, and (c) 182 μs from the beginning of the shock defined as the time of the positive step. These plots also confirm the fact that the observed propagating structures are robust. They extend over a distance of the order of $100\lambda_d$, where λ_d is the Debye length estimated from the electron temperature measured by Langmuir probes. Also apparent in Fig. 4 is the fact that the ion hole is formed before the ion bumps, and the positive bumps excite a wake as they propagate. By varying the duration of the periodic applied pulse, we have observed that the lifetime of the observed phase space structures, estimated from their decay, does not depend on the duration of the pulse. By varying the amplitude of the applied voltage from 0.5 to 16 V, we have also verified that the features reported here remain essentially the same and the observed coherent structures propagate with a velocity that does not depend on the amplitude of the perturbation. This is a rather surprising result. It can be explained by the fact that we are always in a strong nonlinear regime, where subtle ion ballistic effects [30] are completely smeared out. An (x, t) plot of the observed structures clearly shows that they propagate at the acoustic speed obtained by measuring the propagation speed of linear waves.

In conclusion, we have designed a new way to experimentally study ion perturbations propagating in a collisionless plasma by using time resolved laser-induced fluorescence. This gives a powerful tool to investigate ion phase space with unprecedented velocity, space, and time resolution when dealing with repetitive phenomena, either periodic or not.

In order to illustrate how powerful this tool is, we have deliberately chosen experimental situations that have been extensively studied with conventional probe techniques [2,9,10]. In the special case of a step function perturbation, although we have recovered such effects as apparition of forerunner turbulence and precursor ions, our detailed study shows, in the ion space phase, the existence of very complicated and robust long-lived coherent structures extending over a large number of Debye lengths and propagating with approximately the ion acoustic speed. These structures must result from an intricate balance between collisionless dissipative, dispersive, and nonlinear effects. Such results are consistent with what is known about propagation of nonlinear structures in plasmas. The observed self-consistent structures are certainly not of a solitonic nature since their propagation velocity does not depend on their amplitude. Further detailed experimental analysis is under way and will also involve numerical simulation.

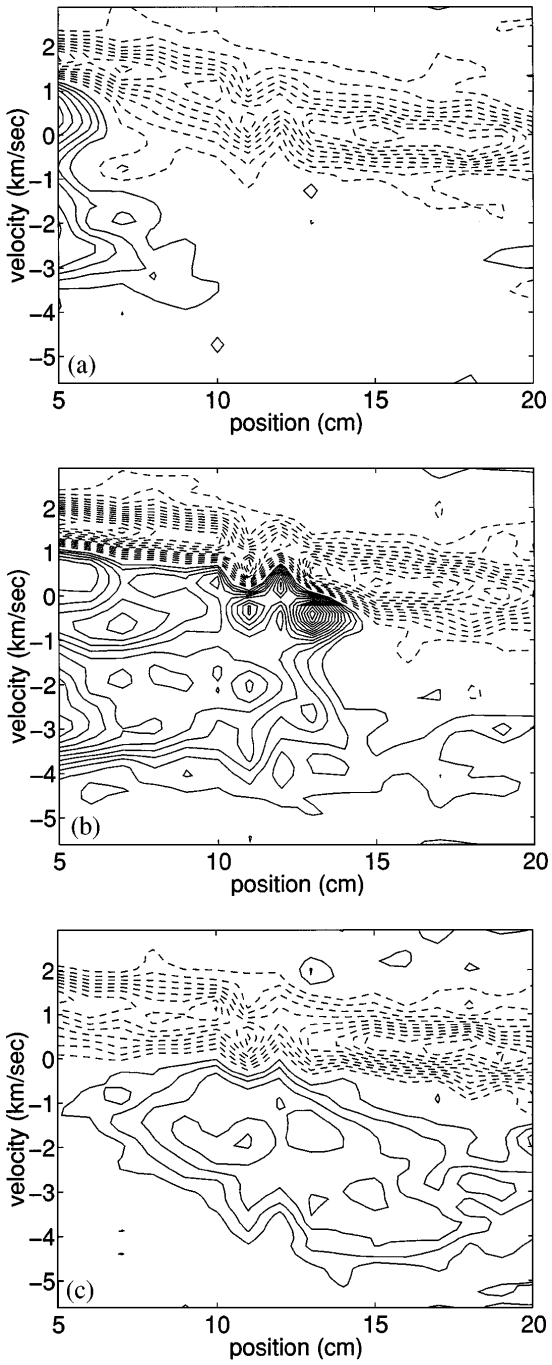

FIG. 4. Contour plots in phase space (x, v) of the perturbation of the ion velocity distribution function measured at time (a) $t = 42$ μs, (b) $t = 82$ μs, and (c) $t = 182$ μs.

The authors are indebted to B. Squizzaro and A. Totin for their skillful technical assistance. They acknowledge stimulating discussions with J. Derouard and N. Sadeghi. Two the authors (F. S. and R. A. S.) were supported by the Ministère des Affaires Etrangères and the Université de Provence, respectively, during their stay in Marseille.

*Permanent address: IPR-UMCP, College Park, MD 20742.
†Permanent address: Department of Physics, University of Colorado, Boulder, CO 80309.

[1] S. S. Moiseev and R. Z. Sagdeev, J. Nucl. Energy C **5**, 43 (1963).
[2] R. J. Taylor, D. R. Baker, and H. Ikezi, Phys. Rev. Lett. **24**, 206 (1970).
[3] A. Y. Wong and R. W. Means, Phys. Rev. Lett. **27**, 973 (1971).
[4] K. V. Roberts and H. L. Berk, Phys. Rev. Lett. **19**, 297 (1967).
[5] M. Kako, T. Taniuti, and T. Watanabe, J. Phys. Soc. Jpn. **31**, 1820 (1971).
[6] P. H. Sakanaka, Phys. Fluids **15**, 1323 (1972).
[7] G. Bonhomme, T. Pierre, G. Leclert, and J. Trulsen, Plasma Phys. Controlled Fusion **33**, 507 (1991).
[8] C. N. Judice, J. F. Decker, and R. A. Stern, Phys. Rev. Lett. **30**, 267 (1973).
[9] R. A. Stern and J. F. Decker, Phys. Rev. Lett. **27**, 1266 (1971).
[10] H. Ikezi, Phys. Fluids **16**, 1668 (1973).
[11] N. Hershkowitz and T. Romesser, Phys. Rev. Lett. **32**, 581 (1974).
[12] H. C. Kim, R. L. Stenzel, and A. Y. Wong, Phys. Rev. Lett. **33**, 886 (1974).
[13] Y. Nakamura, IEEE Trans. Plasma Sci. **10**, 180 (1982).
[14] G. J. Morales and Y. C. Lee, Phys. Rev. Lett. **33**, 1016 (1974).
[15] T. Honzawa, T. Hoshina, and Y. Saito, Phys. Plasmas **2**, 4470 (1995).
[16] V. N. Khudik and I. M. Lansky, Physica (Amsterdam) **85D**, 445 (1995).
[17] G. Thejappa, D. G. Wentzel, R. J. MacDowall, and R. G. Stone, Geophys. Res. Lett. **22**, 3421 (1995).
[18] J. Jolly, J. Phys. III (France) **5**, 1089 (1995).
[19] R. A. Stern and J. A. Johnson, Phys. Rev. Lett. **34**, 1548 (1975).
[20] D. N. Hill, S. Fornaca, and M. G. Wickam, Rev. Sci. Instrum. **54**, 309 (1983).
[21] G. Bachet, L. Chérigier, C. Arnas-Capeau, F. Doveil, and R. A. Stern, J. Phys. III (France) **6**, 1157 (1996).
[22] F. Skiff, G. Bachet, M. Dindelegan, F. Doveil, and R. A. Stern (to be published).
[23] B. Pelissier and N. Sadeghi, Rev. Sci. Instrum. **67**, 3405 (1996).
[24] R. Limpaecher and K. R. McKenzie, Rev. Sci. Instrum. **44**, 726 (1973).
[25] H. Ikezi and R. J. Taylor, Phys. Rev. Lett. **22**, 923 (1969).
[26] M. Carrère, L. Chérigier, C. Arnas-Capeau, G. Bachet, and F. Doveil, Rev. Sci. Instrum. **67**, 4124 (1996).
[27] G. Bachet, L. Chérigier, M. Carrère, and F. Doveil, Phys. Fluids B **5**, 3097 (1993).
[28] F. Anderegg, Ph.D. thesis, Ecole Polytechnique Fédérale de Lausanne, Suisse, 1988.
[29] A. Papoulis, *Probability, Random Variables and Stochastic Processes* (McGraw-Hill, New York, 1984).
[30] I. Alexeff, W. D. Jones, and D. Montgomery, Phys. Rev. Lett. **19**, 422 (1967).